Structural Changes in Solvent-induced Crystallization of Syndiotactic Polystyrene Viewed from the Time-resolved Measurements of Infrared/Raman Spectra and X-ray Diffraction

Kohji Tashiro*, Yoko Ueno, Akiko Yoshioka, Fumitoshi Kaneko, Masamichi Kobayashi

Department of Macromolecular Science, Graduate School of Science, Osaka University, Toyonaka, Osaka 560-0043, Japan

SUMMARY: Solvent-induced crystallization behaviour has been investigated for the glass sample of syndiotactic polystyrene. The time-resolved measurements of the Fourier-transform infrared and Raman spectra and the X-ray diffraction profile revealed the molecular and crystal structural change during the ordering process of polymer chains. On the basis of the idea of critical sequence length, the structural change in the conformational ordering process could be deduced. The crystallization rate was found to be affected remarkably by the kind of solvent: chloroform gave higher crystallization rate than benzene and toluene. This tendency was in contrast to that observed for the gelation process from the dilute solution: the gelation rate was chloroform << benzene. This high contrast between the crystallization and gelation rates could be interpreted qualitatively in terms of the difference in the solubility of polymer in these solvents.

INTRODUCTION

Syndiotactic polystyrene (sPS) is one important species of the polystyrene family, which includes atactic (aPS) and isotactic (iPS). The sPS forms two types of molecular chain conformations in the crystalline region (Ref. 1-11). Roughly speaking, random coils of the glassy state regularize to the planar zigzag form by annealing and to a complex of t_2g_2 form with solvent by absorption of organic solvents. This t_2g_2-solvent complex transfers to the planar zigzag form on removal of the guest solvent by thermal treatment. These changes depend remarkably on the thermal history of the samples, the kind of solvent, etc. Unfortunately, very little has been clarified about the phase transition behavior of the complicated polymorphs of sPS, although a number of studies have been made in order to clarify the characteristic features of these crystalline phases (Ref. 12-21).

In this paper we will trace the solvent-induced crystallization of the glass by comparing the data obtained from the time-resolved FT-IR, FT-Raman, and wide-angle X-ray scattering measurements. The transformation from the glassy state to the crystalline state is intimately

 CCC 1022-1360/99/$ 17.50+.50/0

related with the regularization process of chain segments from the random coil to the conformationally ordered sequence. From such a viewpoint, in order to clarify the transition mechanism of conformational ordering, it is useful to obtain the knowledge about the "critical sequential length" of the IR and Raman bands of sPS chains (Ref. 22). In the second part of this paper an experiment was performed to evaluate the critical sequence lengths of the sPS δ form.

sPS is also known to form a gel with several organic solvents (Ref. 23-29). The cross-linkage parts of the gel are speculated to be basically equivalent to the polymer-solvent complex which is observed in the crystallization phenomenon from the glass to the δ form. An important question is: What relation is there between the solvent-induced crystallization of the glass and the gelation from the dilute solution ? In the third part of this paper, the dependence of the crystallization rate on the type of solvent is investigated and the result is compared with the case of gelation phenomenon from the view-point of polymer-solvent interactions.

EXPERIMENTAL SECTION

Samples

The sPS samples (Mw = 380,000: Mw/Mn = 2.5) were kindly supplied from Idemitsu Kosan Co., Ltd. The films cast from chloroform solution were melted and quenched into liquid nitrogen to prepare the glass (amorphous) samples.

Measurements

In the measurements of the X-ray diffraction and IR and Raman spectra for the samples subjected to the solvent atmosphere, home-made sample cells were used. The measurement was started simultaneously with the solvent injection and the data were saved at constant intervals of time. The infrared spectra were recorded at a resolution of 2 cm^{-1}, using a Bio-Rad FTS-60A FT-IR spectrometer fitted with an MCT detector. Wide angle X-ray diffraction photographs (WAXS) were obtained with graphite-monochromatized Cu-Kα radiation (40kV and 250mA) by using DIP220 of MAC Science Co. Ltd. The FT-Raman spectra were recorded with a Bio-Rad FT-Raman II equipped with a YAG-Nd near-IR laser. The 180° back-scattered light was collected at 2 cm^{-1} resolution.

RESULTS AND DISCUSSION

STRUCTURAL CHANGE IN SOLVENT-INDUCED CRYSTALLIZATION

(A) Time-Resolved FT-IR Spectral Measurement

Fig. 1 shows the time dependence of FTIR spectra taken for the sPS-toluene system. The time dependence of intensity changes of several bands characteristic of the amorphous

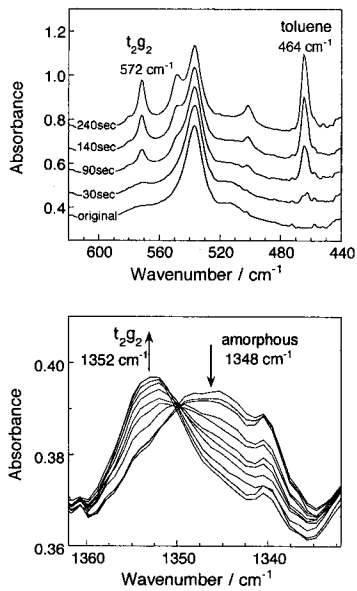

Fig. 1. FTIR spectral changes observed for the glassy sPS exposed to the toluene atmosphere.

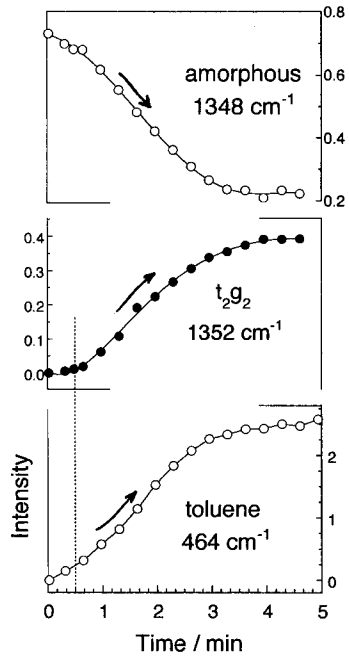

Fig. 2. Time evolution of intensities of IR bands characteristic of each component of sPS.

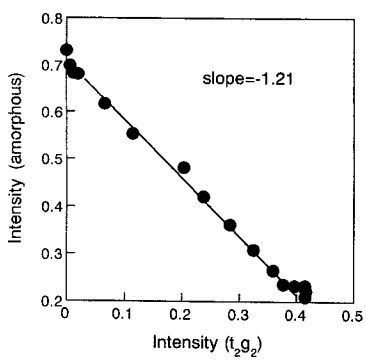

Fig. 3. Plot of IR band intensity of the sPS amorphous component against the band intensity of the t_2g_2 crystalline component.

phase and the t_2g_2 conformation are shown in Fig. 2. After injection of the solvent, the bands of toluene at 464 cm^{-1} began to appear and increased in intensity. After a delay of several tens of seconds, the intensity of the amorphous band (1348 cm^{-1}) began to decrease and the intensity

of the t_2g_2 conformation band (1352 cm^{-1}) increased. This transition ceased in a few minutes. In Fig. 1 an isobestic point was clearly observed, implying that the transition occurs between the two components of the amorphous state and the δ phase. In such a two-component system, the following equations may be applied according to the Lambert-Beer's law:

$$I_A = \varepsilon_A C_A l \qquad \text{and} \qquad I_B = \varepsilon_B C_B l$$

where I_i, ε_i and C_i are the absorbance, molar extinction coefficient and the molar concentration, respectively, of the component i (i = A and B). l is the optical path length. Because $C_A + C_B = 1$, then the following equation is obtained.

$$I_A = -(\varepsilon_A/\varepsilon_B)I_B + \varepsilon_A l \qquad (1)$$

That is to say, a plot of the intensity of the component A against the intensity of the component B should give a straight line with a slope of $-(\varepsilon_A/\varepsilon_B)$. Fig. 3 shows this situation clearly, where the intensity of the t_2g_2 conformation band is plotted against the amorphous band intensity, indicating that the random amorphous phase crystallizes directly into the δ form of the t_2g_2 conformation.

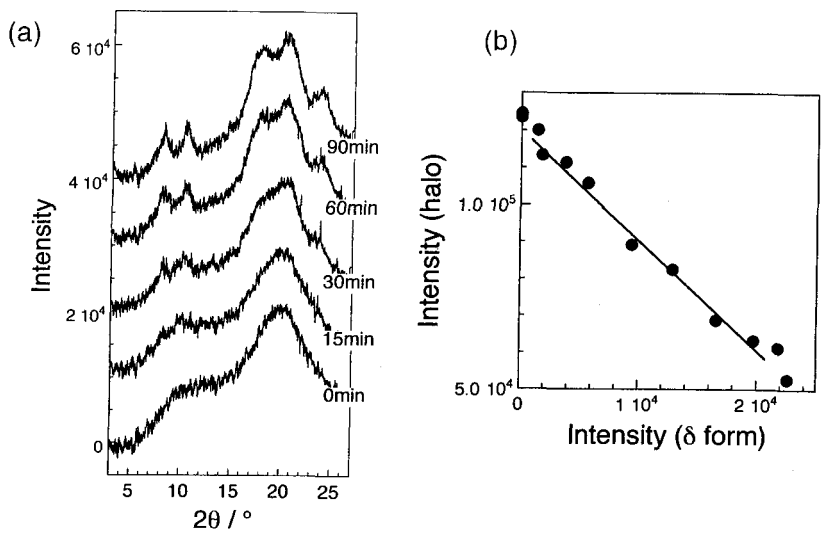

Fig. 4. (a) The change in X-ray diffraction pattern of the sPS glass sample exposed to the toluene atmosphere.

(b) Plot of X-ray scattering intensity of the sPS amorphous component against the intensity of the t_2g_2 crystalline component.

(B) Time-Resolved WAXS Measurement

Fig. 4 (a) shows the time dependence of the X-ray diffraction profile of the glass sample exposed to solvent atmosphere, which was measured by an imaging plate system. The original sample showed the halo pattern characteristic of the amorphous phase. When the solvent was added to the system, the intensity of the reflections characteristic of the δ form increased. As shown in Fig. 4 (b), the intensity of the δ form reflections is plotted against the intensity of the amorphous peak, giving a linear relationship similar to the case for IR band intensity (Fig. 3). This supports also the statement that the amorphous region crystallizes directly into the δ form crystal.

(C) Time-Resolved FT-Raman Spectral Measurement

The Raman spectral changes in several frequency ranges are shown in Fig. 5.

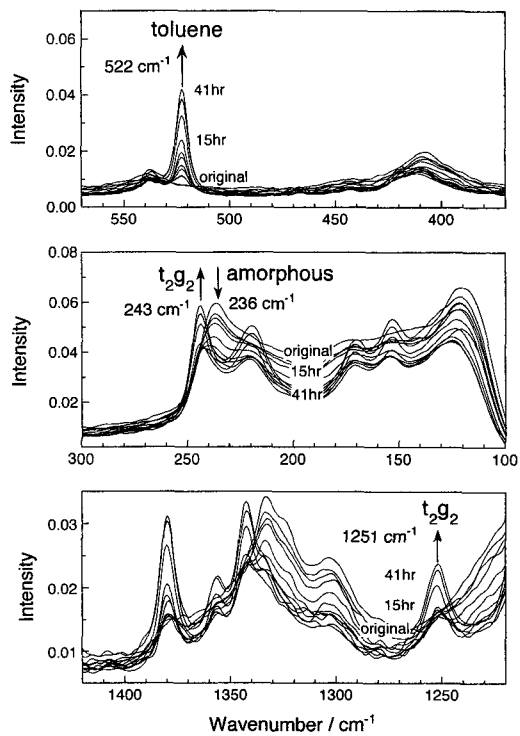

Fig. 5. The FT-Raman spectral changes observed for the glassy sPS sample exposed to the toluene atmosphere.

Fig. 6 shows the time dependence of the intensities evaluated for the Raman bands of toluene at 522 cm^{-1}, the amorphous phase at 236 cm^{-1}, and the t_2g_2 conformation at 243 and 1251 cm^{-1}. The intensity of the toluene band increased immediately after the solvent injection as was seen in the IR measurement. This was followed by the decrease of the amorphous band and the increase of the t_2g_2 conformation bands at 243 cm^{-1}. About 3 hrs after the solvent injection, the intensity of the t_2g_2 band at 1251 cm^{-1} began to increase. (The difference in the time scale among the various data mentioned so far comes from the difference in the thickness of the samples used in each measurement.) In this way, the timing of appearance is different among the bands or the vibrational modes. This difference is considered to come from the difference in the so-called critical sequence length, as discussed in the following section.

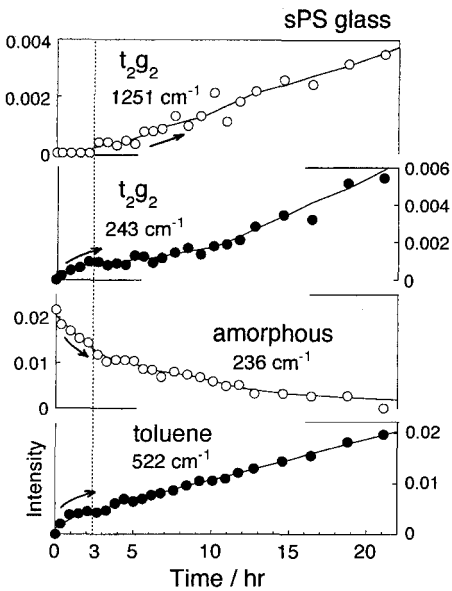

Fig. 6. Time evolution of the Raman band intensity measured for the various components of the sPS sample.

CRITICAL SEQUENCE LENGTH

(A) Concept of Critical Sequence Length

As discussed above, the difference in the timing of appearance of the bands can be attributed to the difference in the critical sequence length. That is to say, the crystalline-sensitive bands have their own critical sequence length (CSL) and do not appear until the regular chain length exceeds the CSL (Ref. 22). The CSL of a band is denoted by a symbol *m*. The *m* value can be evaluated on the basis of the intramolecular isotope-dilution technique. In

this method, random copolymers of the hydrogenous and deuterated monomer units with various compositions are used and their IR/Raman spectra are measured. This method is based on the idea that the oscillation coupling between the neighbouring H (D) monomers is cut off by an insertion of the D (H) species into the chain and the intensity of the H (D) bands is decreased. When the random Markov statistics is assumed for the monomeric sequence along the copolymer chain, the total fraction of the hydrogenous monomer units F(m) with sequential length longer than m is given by

$$F(m) = X^{m-1}[m - (m - 1)X] \qquad (2)$$

where X is the molar fraction of the H species.

The relative intensity R(X) of the band associated with the H species in the copolymer is proportional to F(m).

$$R(X) \propto F(m) \qquad (3)$$

If the band intensity of the pure H (or D) polymer is denoted by R(1.0), then we should have an equation

$$R(X) = F(m)R(1.0)X \qquad (4)$$

The latter part of this equation R(1.0)X indicates that the intensity of pure polymer R(1.0) is reduced by X in the copolymer. Therefore, if we get R(X)/R(1.0) from a series of the observed spectra and plot R(X)/R(1.0) against X, then, we can evaluate the m for the band in question by fitting the observed R(X)/R(1.0) vs X curve to the theoretical curves calculated with the various m values on the basis of equation 4.

(B) Preparation of Random D/H Copolymers of sPS

The sPS copolymers of hydrogenous and deuterated styrenes were synthesized according to the method described by Ishihara *et al*[30] using a Kaminsky-type catalyst (cyclopentadienyl titanium trichloride) and methylaluminoxane in toluene at 40°C. In order to evaluate the m value exactly, the crystallinity and the structural regularity are required to be as high as possible. Therefore, to evaluate the m for the t_2g_2 conformation, we prepared the highly-ordered δ form by exposing the glass sample in the toluene gas atmosphere for a long enough time. The δ form was checked from the X-ray diffraction pattern.

(C) Evaluation of Critical Sequence Length

Figs. 7 and 8 show, respectively, the Raman spectra of the δ form measured for a series of

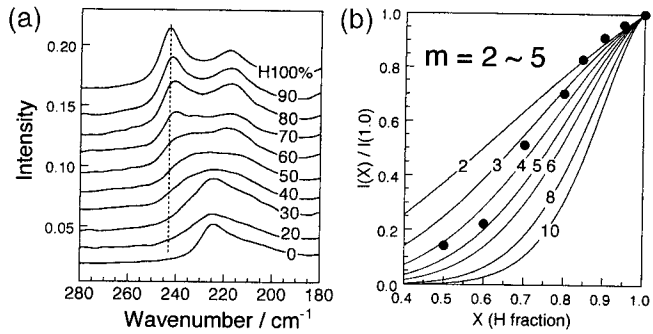

Fig. 7 (a) Raman spectra of the δ form measured for a series of sPS copolymers with various H/D contents (180 - 280 cm^{-1}).
(b) Reduced intensity of the 243 cm^{-1} Raman band plotted against the fraction of the H component. The data are compared with the theoretical curves for the various critical sequence length *m*.

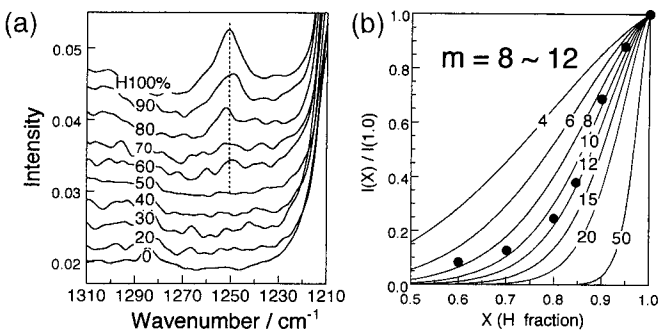

Fig. 8 (a) Raman spectra of the δ form measured for a series of sPS copolymers with various H/D contents (1210 - 13100 cm^{-1}).
(b) Reduced intensity of the 1251 cm^{-1} Raman band plotted against the fraction of the H component. The data are compared with the theoretical curves for the various critical sequence length *m*.

copolymers with different D/H contents. In these figures, the band intensities were normalized by using the band at 622 cm^{-1} as an internal standard. The R(X)/R(1.0) defined in equation 4 was calculated for the different *m* values and compared with the observed data. For example, the intensity of the Raman band at 243 cm^{-1} changes with the D/H content as seen in Fig. 7 (a),

from which the R(X)/R(1.0) was plotted against the H molar fraction X as shown in Fig. 7 (b). By comparing the observed points with the theoretical curves, we could obtain a good fitting of the curves for m = 2 - 5. That is to say, the 243 cm^{-1} band can be detected in the Raman spectra for the first time when 2 - 5 monomers are arranged into a regular t_2g_2 conformation. In the case of the Raman band at 1251 cm^{-1} shown in Fig. 8 (a), the similar analysis revealed the m value of 8 - 12. In other words, about 10 monomeric units must be incorporated into a regular t_2g_2 conformation for the detection of the 1251 cm^{-1} Raman band, corresponding to about 2 repeating periods of the $(t_2g_2)_2$ helical chain or ca. 16 Å along the chain axis.

(C) Detailed Description of Structural Change

Fig. 9 shows the time dependence of the intensities of the IR and Raman bands and the X-ray diffraction measured for the glass sample exposed in the toluene vapor. (In this Fig. the intensities of the IR bands, Raman bands, and X-ray peaks originating from the amorphous region were unified to the same value because these data were collected independently by using the samples with different thickness or with different time-scale of transition.) Immediately after the absorption of toluene, the amorphous phase decreases the intensity and the IR/Raman bands corresponding to the short t_2g_2 conformer (m = 2 - 5) increase in

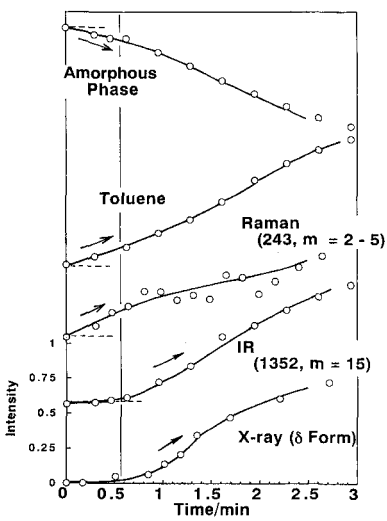

Fig. 9. Time evolution of relative intensities of IR/Raman bands and X-ray scattering measured for the glassy sPS exposed to toluene vapor.

Fig. 10. An illustration of solvent-induced structural development of sPS glass.

intensity. After several tens of seconds, the bands corresponding to longer t_2g_2 conformation (m = 15) begin to appear in the spectra. It should be noticed also that the X-ray scattering peaks can be detected almost at the same timing with these longer t_2g_2 bands. The X-ray scattering can be attained for the first time when the several chain stems are aggregated together and form the crystal lattice.

From Fig. 9, we may describe the structural change occurring in the solvent-induced crystallization of sPS glass as illustrated in Fig. 10. After the injection of toluene, the random coil in the amorphous region begins to regularize partly into the short t_2g_2 chain segments. Furthermore, as the time passes, these short chain segments become longer and gather together to form a kind of cluster. This cluster grows further to give the crystallite of the δ-type structure.

SOLVENT EFFECT ON CRYSTALLIZATION RATE

As discussed above, the sPS crystallizes from the glass state by forming a complex with the absorbed toluene molecules. It may be expected that this crystallization behaviour is affected more or less by the type of organic solvent used. We measured the time dependence of the FTIR spectra for the various organic solvents such as chloroform, benzene and toluene, and compared their crystallization rates. In order to carry out this comparison quantitatively, the film thickness was adjusted to approximately the same value, 30 ± 3 μm.

Fig. 11 shows the FTIR spectral changes measured at room temperature for the different pairs of sPS glass and solvent. The bands characteristic of the used organic solvent and those of the δ crystalline state of the polymer can be detected readily. Fig. 12 shows the time evolution of the crystalline fraction evaluated from the IR spectra shown in Fig. 11. The δ form bands begin to appear after the observation of some induction time, which depends remarkably on which solvent is used. The slope of the curve, i.e., the crystallization rate, is also different. The chloroform solvent shows the shortest induction period and the highest crystallization rate among the three sample systems. When a mixture of chloroform and benzene (or toluene) was used, the crystallization rate was in between those observed for the pure solvents. That is to say, the crystallization rate observed for pure benzene or toluene was accelerated by adding chloroform; or, in other words, the crystallization rate observed for pure chloroform was reduced by adding benzene or toluene.

RELATION BETWEEN CRYSTALLIZATION AND GELATION

Kobayashi et al. evaluated the gelation rate of sPS dilute solutions by the time-resolved FTIR measurement for various kinds of solvent such as benzene, chloroform, and

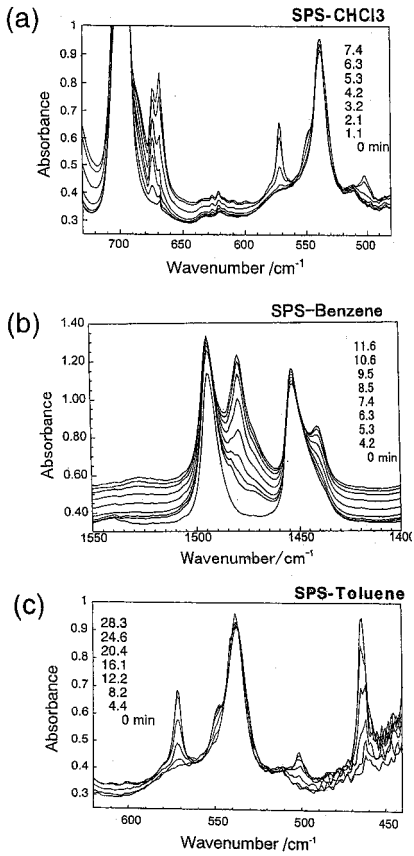

Fig. 11. Infrared spectral changes during the crystallization of the glassy sPS samples exposed to the various kinds of solvent. (a) chloroform, (b) benzene and (c) toluene.

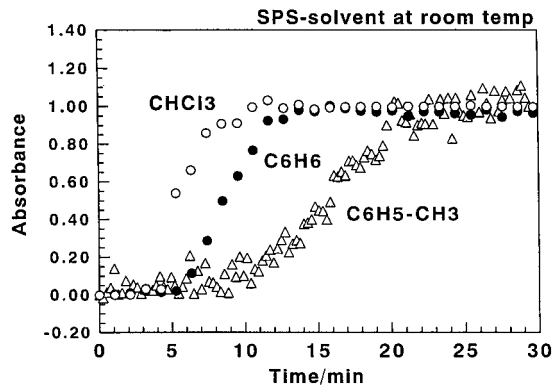

Fig. 12. Time evolution of the crystallinity of the glassy sPS samples exposed to the various solvents. (a) chloroform, (b) benzene, and (c) toluene.

carbon tetrachloride (Ref. 27). The chloroform causes quite slow gelation compared with benzene or carbon tetrachloride. This difference in the gelation rate between chloroform and benzene is in contrast to the difference in the solvent-induced crystallization rate as mentioned above. The effect of a mixture of solvents on the gelation rate is similar to that observed for the crystallization phenomenon, in the sense that an addition of the solvent giving slower gelation (or crystallization) accelerates the change remarkably. That is to say, we have the following relation:

Gelation	$CHCl_3 < CHCl_3 + C_6H_6 < C_6H_6$
Crystallization	$CHCl_3 > CHCl_3 + C_6H_6 > C_6H_6$

Why is such a quite contrast tendency observed between the gelation and crystallization phenomena ? It may be possible to interpret this difference qualitatively in terms of the solubility of sPS for these different kinds of solvent. In the crystallization process from the glass at room temperature, the polymer segments must move and be arranged into the regular packing structure. The polymer chain segments in the glassy state are originally frozen below the glass transition temperature, but their mobility can be enhanced by the penetration of solvent molecules. That is to say, the solvent dissolves the polymer chains even partly in the glassy state and plays a role as a kind of plasticizer. Therefore the solvent giving higher solubility of sPS is considered to give the higher crystallization rate. On the other hand, the gelation causes the formation of cross linkages which are considered to be equivalent essentially to the crystalline state of sPS-solvent complex. In the dilute solution the random coils are dipped in the sea of solvent and are surrounded by many solvent molecules. However, in order to form the cross-linkages or the stoichiometric polymer-solvent complex, the surplus solvent molecules must be purged out of the random coils. That is to say, the solvent with lower solubility tends to result more easily in the formation of cross-linkage parts. In other words, the solvent system with the higher solubility may give the slower gelation process.

Therefore, the difference in the solubility of solvents can allow us to interpret qualitatively the difference in the complex formation rate between the gelation and the crystallization. At room temperature the sPS is more easily dissolved in chloroform than in benzene. Therefore we may expect the following tendency, which corresponds well to the observed results.

Solubility	$CHCl_3 > C_6H_6$
Crystallization	$CHCl_3 > C_6H_6$
Gelation	$CHCl_3 < C_6H_6$

The interactions between sPS and organic solvent molecules seem to play a quite important role in the formation process of gel and crystal, although they work oppositely in these two transition phenomena.

ACKNOWLEDGMENT

The authors deeply thank the Idemitsu Kosan Co., Ltd. for supplying sPS samples.

REFERENCES

(1) Y. Chatani, Y. Shimane, Y. Inoue, T. Inagaki, T. Ijitsu, T. Yukinari, *Polymer* **33**, 488 (1992).
(2) Y. Chatani, Y. Shimane, T. Inagaki, T. Ijitsu, T. Yukinari, *Polymer* **34**, 1625 (1993).
(3) G. Guerra, V. Vincenzo., M. Vitagliano, C. De Rosa, V. Petraccone, P. Corradini, *Macromolecules* **23**, 1539 (1990).
(4) C. De Rosa, M. Rapacciuolo, G. Guerra, V. Petraccone, P. Corradini, *Polymer* **33**, 1423 (1992).
(5) Y. Chatani, Y. Shimane, T. Inagaki, T. Ijitsu, T. Yukinari, H. Shikuma, *Polymer* **34**, 1620 (1993).
(6) C. De Rosa, *Macromolecules* **29**, 8460 (1996).
(7) P. Corradini, C. De Rosa, G. Guerra, R. Napolitano, V. Petraccone, B. Porozzi. *Eur. Polym. J.* **30**, 1173 (1994).
(8) M. Tosaka, N. Hamada, M.Tsuji, S. Kohjiya, T. Ogawa, S. Isoda, T. Kobayashi, *Macromolecules* **30**, 4132 (1997).
(9) N. Hamada, M. Tosaka, M. Tsuji, S. Kohjiya, K. Katayama, *Macromolecules* **30**, 6888 (1997).
(10) M. Tosaka, N. Hamada, M. Tsuji, S. Kohjiya, *Macromolecules* **30**, 6592 (1997).
(11) S. J. Spell, Makromol. Symp., **114**, 63 (1997).
(12) C.D e Rosa, G. Guerra, V. Petraccone, P. Corradini, *Polym. J.* **23**, 1435 (1991).
(13) E. J. Kellar, C. Galiotis, E. D. Andrews, *Macromolecules* **29**, 3515 (1996).
(14) E. J. Kellar, A. M. Evans, J. Knowles, C. Galiotis, E. D. Andrews, *Macromolecules* **30**, 400 (1997).
(15) N. M. Reynolds and H. D. Stidham, S. L. Hsu, *Macromolecules* **24**, 3662 (1991).
(16) N. M. Reynolds, S. L. Hsu, *Macromolecules* **23**, 3463 (1990).
(17) R. A. Nyquist, C. L. Putzig, M. A. Leugers, R. D. McLachlan, B. Thill, *Appl. Spectrosc.* **46**, 981 (1992).
(18) P. Musto, S. Tavone, G. Guerra, C. De Rosa, *J. Polym. Sci., Polym. Phys.* **35**, 1055 (1997).
(19) C. G. Zimba, J. F. Rabolt, *Macromolecules* **22**, 2867 (1989).
(20) M. Kobayashi, T. Nakaoki, N. Ishihara, *Macromolecules* **22**, 4377 (1989).
(21) M. Kobayashi, T. Nakaoki, N. Ishihara, *Macromolecules* **23**, 78 (1990).
(22) M. Kobayashi, K. Akita, H. Tadokoro, *Makromol. Chem.* **118**, 324 (1968).

(23) M. Kobayashi, T. Yoshioka, T. Kozasa, J. Suzuki, S. Funahashi, Y. Izumi, *Macromolecules* **27**, 1349 (1994).
(24) M. Kobayashi, T. Yoshioka, M. Imai, Y. Itoh, *Macromolecules* **28**, 7376 (1995).
(25) M. Kobayashi, T. Nakaoki, *J. Mole. Struc.* **242**, 315 (1991).
(26) M. Kobayashi, T.Kozasa, *Appl. Spec.* **47**, 1417 (1993).
(27) M. Kobayashi, *Makromol. Symp.*, **114**, 1 (1997).
(28) J. M. Guenet, *Makromol. Symp.*, **114**, 97 (1997).
(29) C. Daniel, A. Menelle, A. Brulet, and J. M. Guenet, *Makromol. Symp.*, **114**, 159 (1997).
(30) N. Ishihara, T. Seimiya, K. Kuramoto, and M. Uoi, *Macromolecules*, **19**, 2464 (1986).

* * * * * *

To readers:

One of our co-authors, Dr. Masamichi Kobayashi, emeritus professor of Osaka University, passed away at the age of 64 on the 1st day of the last April. We would like to dedicate this paper to him and pray for the repose of his soul.

K. T.